Ji et al. Cell Division (2024) 19:25
https://doi.org/10.1186/s13008-024-00129-7

Cell Division

RESEARCH Open Access

Long non-coding RNA NEAT1 induced by BHLHE40 activates Wnt/β-catenin signaling and potentiates colorectal cancer progression

Anlong Ji[1†], Hui Li[2†], Xiangwei Fu[1], Yourong Zhang[1] and Yanhe Liu[1*]

Abstract

Background Nuclear-enriched abundant transcript 1 (NEAT1), a long noncoding RNA (lncRNA), has been implicated in the colorectal cancer (CRC) progression. However, its upstream mechanism has not been well studied. In the present study, the functions and mechanisms of NEAT1 in CRC were investigated.

Methods The NEAT1 expression in CRC tissues and CRC cells was analyzed by RT-qPCR. The genes co-expressed with NEAT1 in CRC were obtained from UALCAN, which were intersected with the transcription factors targeting NEAT1 from hTFtarget. Dual-luciferase assay, RT-qPCR, and ChIP were conducted to analyze the transcriptional regulatory relationship between BHLHE40 and NEAT1. LoVo and HCT-15 cells knocking down BHLHE40 and overexpressing NEAT1 were subjected to MTT, Transwell, Western blot, and flow cytometry to examine the malignant aggressiveness of CRC cells. The effects of knocking down BHLHE40 and overexpressing NEAT1 on tumor and lung metastasis were investigated in mice using HE and immunohistochemical analyses.

Results NEAT1 and BHLHE40 were significantly overexpressed in CRC tissues and cells. BHLHE40 has a binding relationship with the NEAT1 promoter. Knockdown of BHLHE40 resulted in a reverted malignant phenotype in vitro and slowed tumor growth and metastasis dissemination in *vivo*, which were reversed by NEAT1 overexpression. Overexpression of BHLHE40 increased Wnt/β-catenin pathway activity, but knockdown of NEAT1 decreased Wnt/β-catenin pathway activity.

Conclusions BHLHE40 mediates the transcriptional activation of NEAT1, which activates the Wnt/β-catenin pathway and promotes the CRC progression.

Keywords Long noncoding RNA NEAT1, BHLHE40, Transcription, Colorectal cancer, Wnt/β-catenin pathway

Background

Colorectal cancer (CRC) accounts for about 10% of all annually diagnosed cancers and cancer-related deaths in the world range [1]. Due to improvements in treatment regimens, including colectomy, chemotherapy, and immunotherapy, the overall 5 year survival for CRC patients is approximately 64% [2]. However, more than one-half of all diagnoses and deaths are attributable to modifiable risk factors, such as smoking, an unhealthy diet, alcohol overconsumption, physical inactivity, and excess body weight [3]. Even though inherited genetic

[†]Anlong Ji and Hui Li have contributed equally to this work.

*Correspondence:
Yanhe Liu
liuyanhe7191@163.com
[1] Department of General Surgery, The Second Affiliated Hospital of Hainan Medical University, No. 368, Yehai Avenue, Haikou 570216, Hainan, People's Republic of China
[2] Department of Geriatrics, The Second Affiliated Hospital of Hainan Medical University, No. 368, Yehai Avenue, Haikou 570216, Hainan, People's Republic of China

susceptibility has a vital role in some CRC cases, the majority of CRC cases are sporadic and non-inherited [4]. Therefore, elucidating the molecular mechanisms behind the development and progression of CRC is of crucial importance. Epithelial-mesenchymal transition (EMT) is a process during which cells lose their epithelial characteristics and gain mesenchymal properties, and EMT has an indispensable role in tumor progression and metastasis in CRC [5]. Hence, the exploration of biomolecules related to EMT is helpful for the treatment of CRC.

Noncoding RNAs (ncRNA) are a group of transcripts that are coded by the genome but are generally not translated into proteins [6]. Among them, long ncRNAs (lncRNAs) play key roles in mediating chromatin dynamics, gene expression, growth, and development of cancers, including CRC [7]. LncRNAs have been summarized to control cell proliferation, cell migrative, and invasive ability, as well as EMT in CRC [8]. The nuclear-enriched abundant transcript 1 (NEAT1) is a lncRNA that is enhanced in various human cancers and encourages cell growth, migration, and invasion [9]. For instance, NEAT1 has been reported to promote melanoma progression by activating EMT and immune responses [10]. More relevantly, NEAT1 has been verified to participate in CRC development and progression by acting as a competing endogenous RNA [11]. Interestingly, NEAT1 has been verified to activate the Wnt/β-catenin signaling to promote the progression of CRC and osteoarthritis [12, 13]. Indeed, the Wnt signaling pathway is closely related to cancer cell proliferation, heterogeneity, and EMT/migration/invasion/metastasis [14, 15]. Therefore, we also wondered whether the effects of NEAT1 on EMT in CRC were elicited through the Wnt/β-catenin signaling. In addition, NEAT1 expression has been revealed to be regulated by a signal transducer and activator of transcription 3, a transcription factor [16]. According to this finding, we anticipated that the expression of NEAT1 in CRC was controlled by a transcription factor. Class E basic helix-loop-helix protein 40 (BHLHE40) was thus identified as an upstream modifier of NEAT1 in the present study using an integrated bioinformatics prediction. Based on the above reports, we explored here the role and mechanism of NEAT1 in the EMT of CRC.

Results

High expression of NEAT1 is identified in CRC tissues and cells

By UALCAN (http://ualcan.path.uab.edu/index.html), we verified the high expression of NEAT1 in patients with colon adenocarcinoma (COAD) and rectum adenocarcinoma (READ) (Fig. 1A). RT-qPCR analysis showed that NEAT1 expression was significantly upregulated in CRC tissues relative to their adjacent tissues (n = 54) (Fig. 1B). Consistently, NEAT1 expression was higher in CRC cell lines than that in HCoEpiC cells (n = 3) (Fig. 1C).

BHLHE40 mediates the transcription of NEAT1 in CRC cells

To investigate the upstream mechanisms responsible for high NEAT1 expression in CRC, we obtained genes co-expressed with NEAT1 in both COAD and READ in UALCAN (positively correlated genes, heatmaps show the top 25 genes with the highest correlation) (Fig. 2A). These genes were intersected with the transcription factors targeting NEAT1 downloaded from hTFtarget (http://bioinfo.life.hust.edu.cn/hTFtarget/#!/). There were 8 intersecting transcription factors: BHLHE40, EGR1, CCNT2, FOS, BTAF1, ZNF236, EZH1, and DDX5 (Fig. 2B). The expression of these eight transcription factors in CRC was analyzed in UALCAN, and the results are presented in Fig. 2C. Among the transcription factors, only BHLHE40 was highly expressed in both COAD and READ (Fig. 2D). We therefore hypothesized that BHLHE40, which is highly expressed in CRC, is the key reason for the high expression of NEAT1 in CRC, and selected BHLHE40 as a potential regulator of NEAT1 for further analysis.

The binding fragment of BHLHE40 on the NEAT1 promoter with the highest score was obtained from hTFtarget (Fig. 2E). RT-qPCR detected significant high expression of BHLHE40 in the CRC tissues (n = 54) and cells (n = 3) (Fig. 2F, G). LoVo cells and HCT-15 cells with relatively higher BHLHE40 expression were infected with lentivirus sh-BHLHE40 1#, 2#, and 3#, and sh-BHLHE40 1# with the best infection efficiency was selected for the following assays (Fig. 2H). Significantly reduced NEAT1 expression was observed using RT-qPCR after the knockdown of BHLHE40 in LoVo and HCT-15 cells (Fig. 2I). According to the dual luciferase activity assay, the knockdown of BHLHE40 contributed to a significant reduction in NEAT1 transcription and a decrease in luciferase activity (Fig. 2J). In addition, ChIP assays were performed as well, and the results showed that BHLHE40 bound to the promoter region of NEAT1 in CRC cells (Fig. 2K).

Silencing of BHLHE40 reverts the malignant phenotype of CRC cells via NEAT1

To investigate whether the involvement of BHLHE40 in CRC progression was elicited through NEAT1, we conducted rescue experiments by overexpressing NEAT1 after knocking down BHLHE40 in LoVo and HCT-15 cells. RT-qPCR results showed that the infection of NEAT1 overexpression was successful (Fig. 3A). MTT assay showed a significant decrease in cell viability in sh-BHLHE40-transfected LoVo and HCT-15 cell lines, but overexpression of NEAT1 increased cell viability

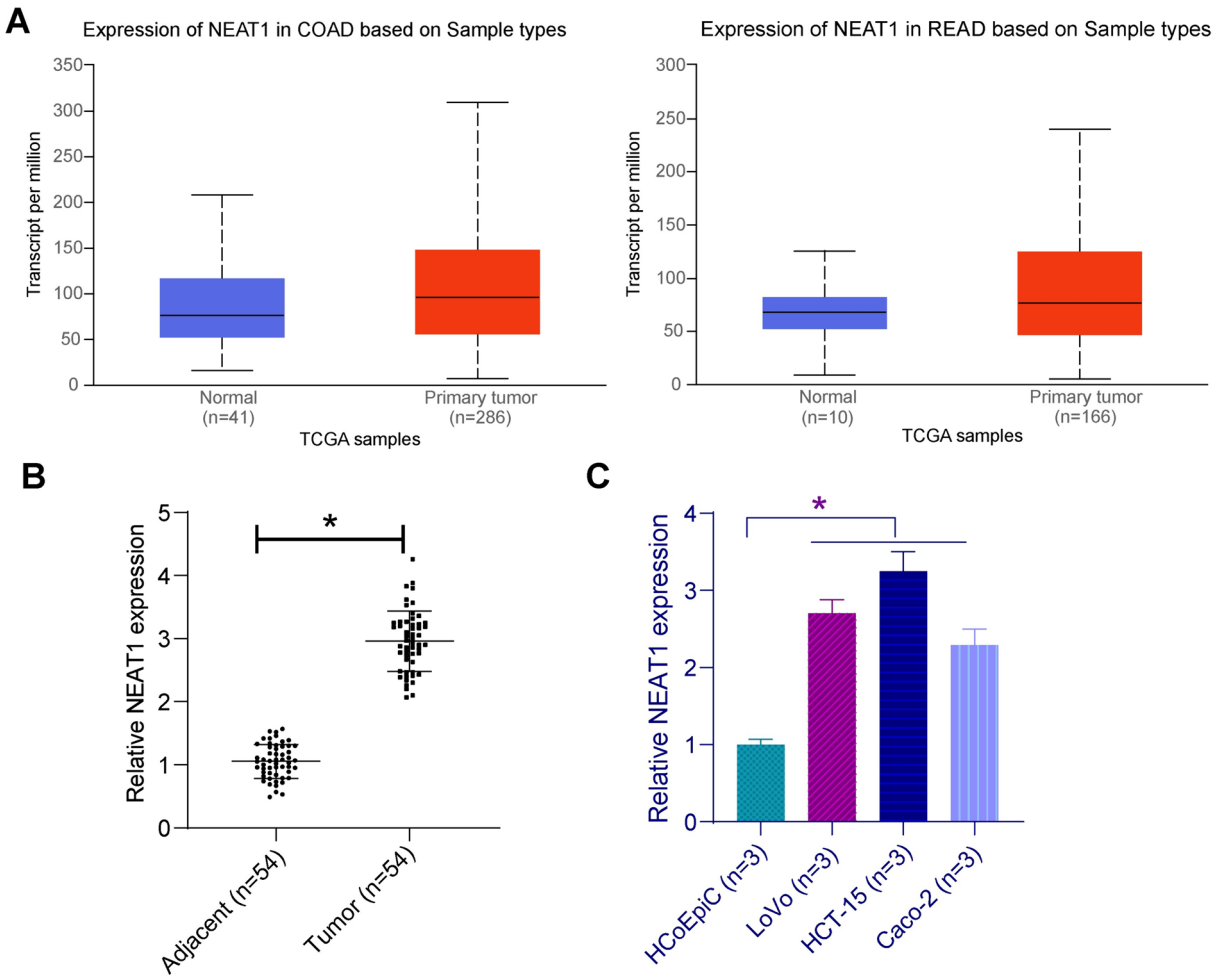

Fig. 1 NEAT1 is highly expressed in human CRC tissues and cell lines. **A** High expression of NEAT1 in COAD and READ patients in UALCAN. **B** Detection of NEAT1 expression in CRC tissues and adjacent tissues by RT-qPCR (n = 54). **C** Expression of NEAT1 in CRC cell lines and HCoEpiC cells by RT-qPCR. Results were expressed as magnitude of relative expression (means ± SD) from three independent experiments. **B** Paired t-test; **C** one-way ANOVA. *$p < 0.05$

(Fig. 3B). Transwell assays showed that depletion of BHLHE40 resulted in a significant reduction in cell migration and invasion, but oe-NEAT1 promoted cell migration and invasion (Fig. 3C, D). It was found by western blot assays that knockdown of BHLHE40 resulted in elevated levels of E-cadherin and reduced levels of N-cadherin and Vimentin in cells, and overexpression of NEAT1 promoted the EMT event (Fig. 3E). Finally, CRC cell apoptosis was evaluated using flow cytometry. We observed elevated apoptosis in BHLHE40-silenced cells and inhibition of apoptosis by oe-NEAT1 (Fig. 3F).

Depletion of BHLHE40 slows tumor growth and lung metastasis via NEAT1

We then performed in vivo experiments by injecting HCT-15 cells after infection into nude mice subcutaneously. The sh-BHLHE40 group demonstrated significantly inhibited tumor growth compared to the sh-NC group, but oe-NEAT1 significantly promoted tumor growth (Fig. 4A). It was observed using immunohistochemical analysis that BHLHE40 and Ki-67 expression was significantly reduced in tumor tissues in the sh-BHLHE40 group, and NEAT1 increased the expression of Ki-67 without the alteration of BHLHE40 (Fig. 4B). We also injected HCT-15 cells after infection into the tail veins of mice to evaluate metastasis in vivo. HE staining showed that the sh-BHLHE40 group had reduced lung metastasis and NEAT1 increased lung metastasis (Fig. 4C). Western blot detected that sh-BHLHE40 inhibited the expression of BHLHE40 as well as metastasis-associated markers Vimentin, and N-cadherin, and promoted the expression of E-cadherin

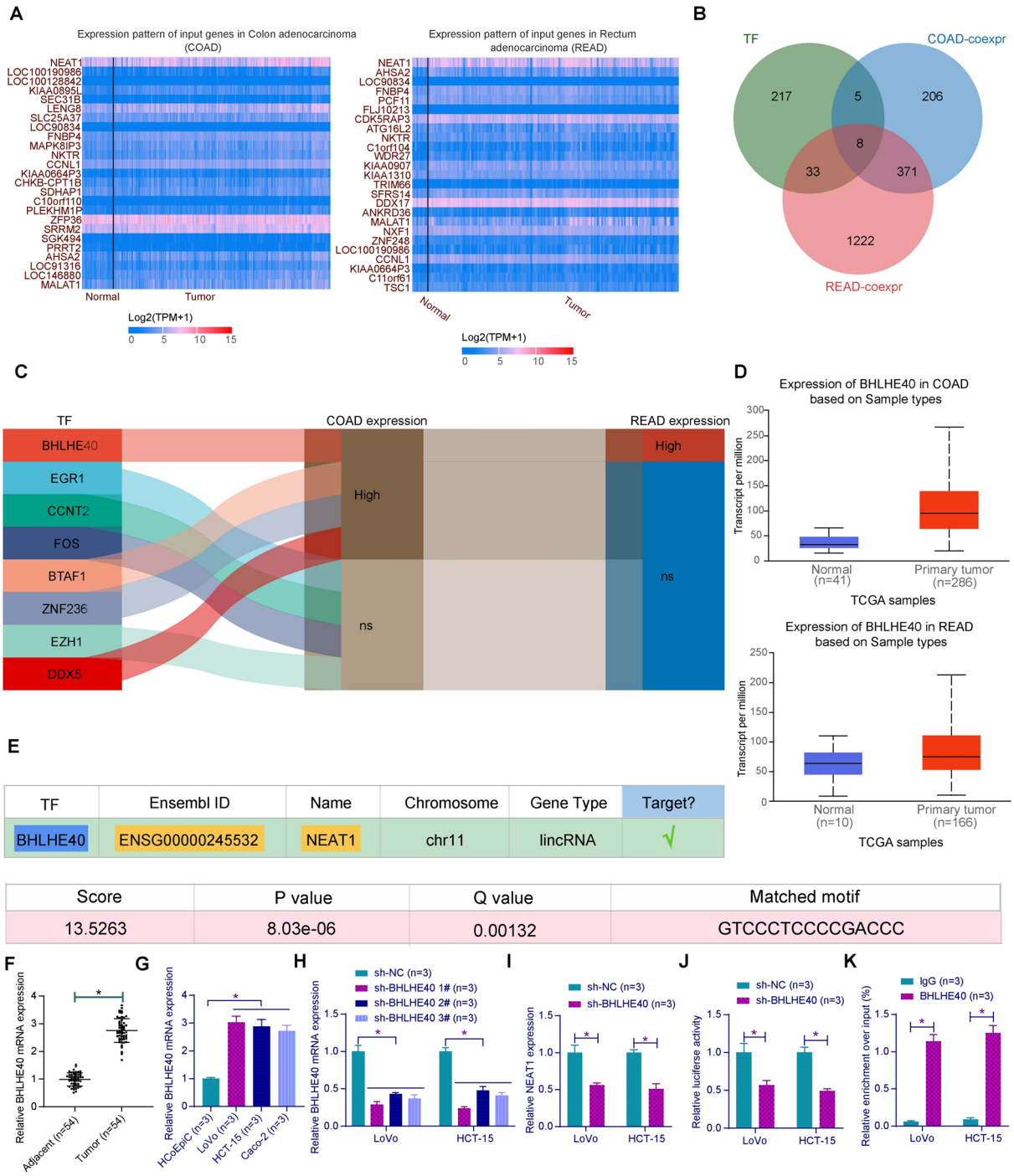

Fig. 2 BHLHE40 mediates the transcription of NEAT1 in CRC cells. **A** Genes co-expressed with NEAT1 in CRC were obtained from UALCAN. **B** The intersection of genes co-expressed with NEAT1 in COAD and READ and the transcription factors targeting NEAT1 downloaded from hTFtarget. **C** The expression of these eight transcription factors in CRC was analyzed in the UALCAN. **D** The expression of BHLHE40 in both COAD and READ. **E** The binding fragment of BHLHE40 on the NEAT1 promoter with the highest score. **F** RT-qPCR detection of BHLHE40 expression in CRC tissues and adjacent tissues by RT-qPCR (n = 54). **G** Expression of NEAT1 in CRC cell lines and HCoEpiC cells by RT-qPCR. **H** Knockdown efficiency of BHLHE40 by RT-qPCR. **I** RT-qPCR detection of NEAT1 expression after knockdown of BHLHE40 in LoVo and HCT-15 cells. **J** Changes in luciferase activity after knockdown of BHLHE40 using luciferase activity assay. **K** BHLHE40 binding to the NEAT1 promoter in CRC cell using ChIP assay. Results were expressed as magnitude of relative expression (means ± SD) from three independent experiments. **F** Paired t-test; **G** one-way ANOVA; **H**–**K** two-way ANOVA. *$p < 0.05$

in lung-infiltrating tumor tissues (Fig. 4D). By contrast, overexpression of NEAT1 resulted in diminished expression of E-cadherin and increased expression of Vimentin and N-cadherin (Fig. 4D).

BHLHE40 mediates NEAT1 transcription to activate the Wnt/β-catenin pathway

Western blot was conducted to examine the expression of EMT- and the Wnt/β-catenin pathway-related proteins in response to oe-BHLHE40 (oe-NC as control) or oe-BHLHE40 + sh-NEAT1 (oe-BHLHE40 + sh-NC as control). Overexpression of BHLHE40 promoted the activation of Wnt/β-catenin signaling and EMT, while knockdown of NEAT1 significantly impaired the Wnt/β-catenin signaling and suppressed EMT in the presence of oe-BHLHE40 (Fig. 5A).

We treated CRC cells overexpressing BHLHE40 with the Wnt/β-catenin antagonist iCRT3. The result of the TOP/FOP flash assay demonstrated a significant enhancement of luciferase activity in TOP flash/FOP flash in cells overexpressing BHLHE40, indicating that the Wnt/β-catenin pathway was activated, while iCRT3 significantly inhibited Wnt/β-catenin pathway activity (Fig. 5B). Overexpression of BHLHE40 significantly promoted the proliferative activity of CRC cells, whereas iCRT3 decreased the proliferative activity of the cells (Fig. 5C). It was observed using the Transwell assay that overexpression of BHLHE40 enhanced cell migration and invasion activity, while iCRT3 inhibited the migration and invasion of CRC cells (Fig. 5D, E). Similarly, BHLHE40 inhibited apoptosis in CRC cells, while blocking the Wnt/β-catenin pathway restored apoptosis in CRC cells (Fig. 5F).

Discussion

LncRNAs play a central role in CRC growth and metastasis, and existing reports focus mainly on their role as competitive endogenous RNAs by occupying the shared binding sequences of miRNAs, thus manipulating the expression of their downstream target genes [17]. Herein, we discovered that NEAT1 expression was elevated by the oncogenic transcription factor BHLHE40 in CRC. Silencing of BHLHE40 inhibited viability and EMT in CRC cells, and reduced tumor growth and lung metastasis. Furthermore, we confirmed that overexpression of NEAT1 can overturn the anti-tumor effects of sh-BHLHE40. Finally, we substantiated that the activated Wnt/β-catenin pathway by BHLHE40 was blocked again by the depletion of NEAT1.

NEAT1 has been identified as a significantly upregulated lncRNA in cervical cancer tissues, and overexpression of NEAT1 was associated with worse survival in patients with cervical cancer [18]. Consistently, we validated the upregulation of NEAT1 in CRC tissues and cells. Regarding its upstream mechanism, NEAT1 overexpression has been linked to N6-methyladenosine modification in prostate cancer [19]. We corroborated here that the oncogenic transcription factor BHLHE40 was responsible for the upregulation of NEAT1 in CRC. BHLHE40 (also known as BHLHB2/DEC1/SHARP2/STRA13) has a poorly understood potential for transcriptional induction [20]. The most recent study also indicated that BHLHE40 could directly modulate INHBA expression, thereby involving the progression of CRC [21]. We obtained the binding site between BHLHE40 and the NEAT1 promoter from the bioinformatics website and corroborated their physical binding using dual-luciferase and ChIP assays.

BHLHE40 mRNA and protein expression were found to be strongly induced by hypoxia or serum starvation in pancreatic cancer cell lines [22]. More relevantly, BHLHE40 was expressed at a much higher level in CRC than in the adjacent normal tissues, and CRC patients with higher BHLHE40 expression had a shorter survival time [23]. In the present study, we not only demonstrated the overexpression of BHLHE40 in human CRC tissues and cell lines but also found that the depletion of BHLHE40 using shRNA successfully reduced the malignant aggressiveness of CRC cells in vitro and in vivo. BHLHE40 silencing by siRNA has been reported to suppress tumor cell invasion of MCF-7 cells [24]. In the context of hepatocellular carcinoma, overexpression of BHLHE40 promoted EMT by losing epithelial protein and regaining mesenchymal proteins, while effectively antagonizing the impact of 8-Methoxypsoralen on EMT [25]. Furthermore, Sethuraman et al. revealed that BHLHE40 knockdown significantly reduced primary tumor growth and lung metastases in orthotopic xenograft and metastasis models of breast cancer by inducing HBEGF transcription [26]. Mechanistically, BHLHE40

(See figure on next page.)

Fig. 3 NEAT1 reverses the anti-tumor effects of sh-BHLHE40 in CRC cells. **A** RT-qPCR detection of NEAT1 overexpression efficiency. **B** MTT assay for LoVo and HCT-15 cell viability. **C** Transwell assay for LoVo and HCT-15 cell migration ability. **D** Transwell assay for LoVo and HCT-15 cell invasion ability. **E** Western blot for E-cadherin, N-cadherin, and Vimentin expression in LoVo and HCT-15 cells. **F** Flow cytometry for LoVo and HCT-15 cell apoptosis. Results were expressed as magnitude of relative expression (means ± SD) from three independent experiments. **A**–**F** two-way ANOVA. $^{*}p < 0.05$

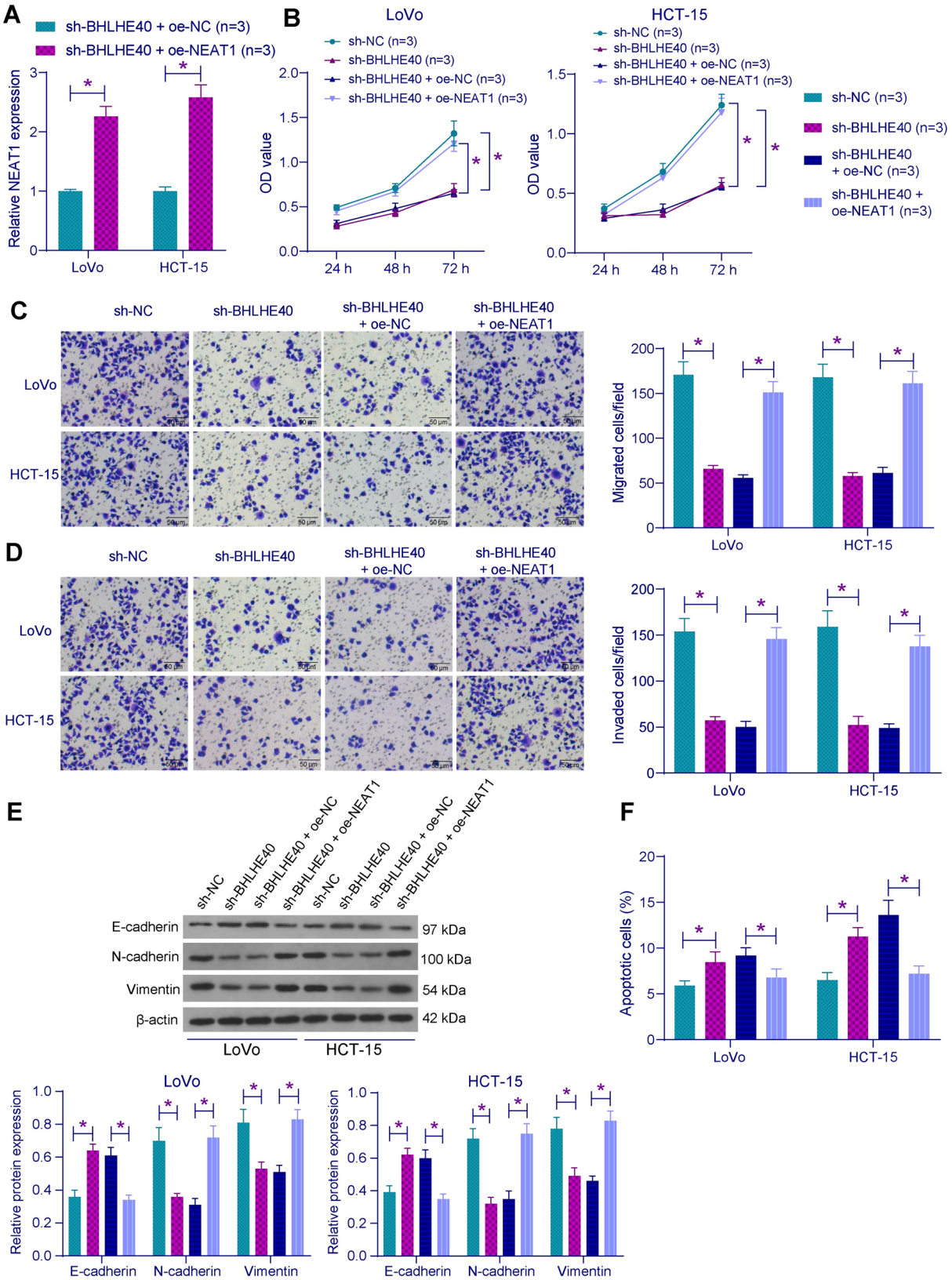

Fig. 3 (See legend on previous page.)

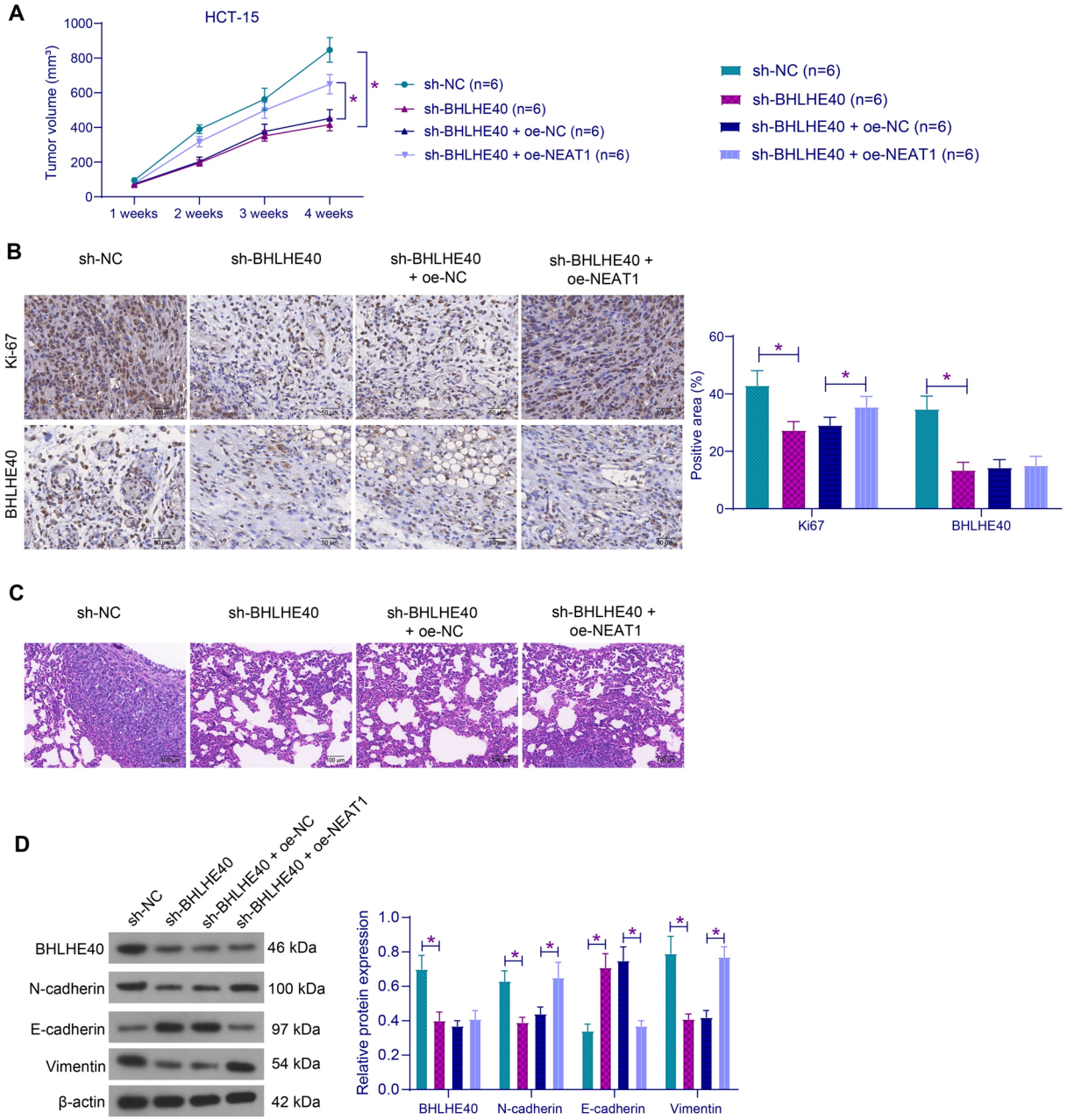

Fig. 4 NEAT1 reverses the metastasis-suppressing and tumor-suppressing properties of sh-BHLHE40. HCT-15 cells after infection were injected subcutaneously into nude mice to observe tumor growth. **A** Tumor growth curve. **B** Immunohistochemical analysis of BHLHE40 and Ki67 expression in xenograft tumor tissues of nude mice. **C** HCT-15 cells after infection were injected into nude mice via the tail vein, and lung metastasis formation was observed using HE staining. **D** Western blot for BHLHE40 and EMT-related protein expression in metastatic tissues with lung infiltration. Results were expressed as magnitude of relative expression (means ± SD) from six nude mice in each group. Two-way ANOVA. *$p < 0.05$

expression was induced by TGF-β in pancreatic cancer cells and modulated the nuclear, cytoplasmic, or membrane localization of EMT-associated factors, including snail, claudin-4 as well as N-cadherin [27]. Here, the evidence derived from our rescue experiments displayed that NEAT1 was the downstream effector of BHLHE40 in CRC. In the same vein, silencing of NEAT1 enhanced the apoptosis and suppressed the invasion of CRC cells [28]. As for its role in EMT, the downregulation of NEAT1 can reverse the EMT of gemcitabine-resistant pancreatic cancer cells by reducing the expression of ZEB2 [29]. However, we cannot exclude the involvement of other

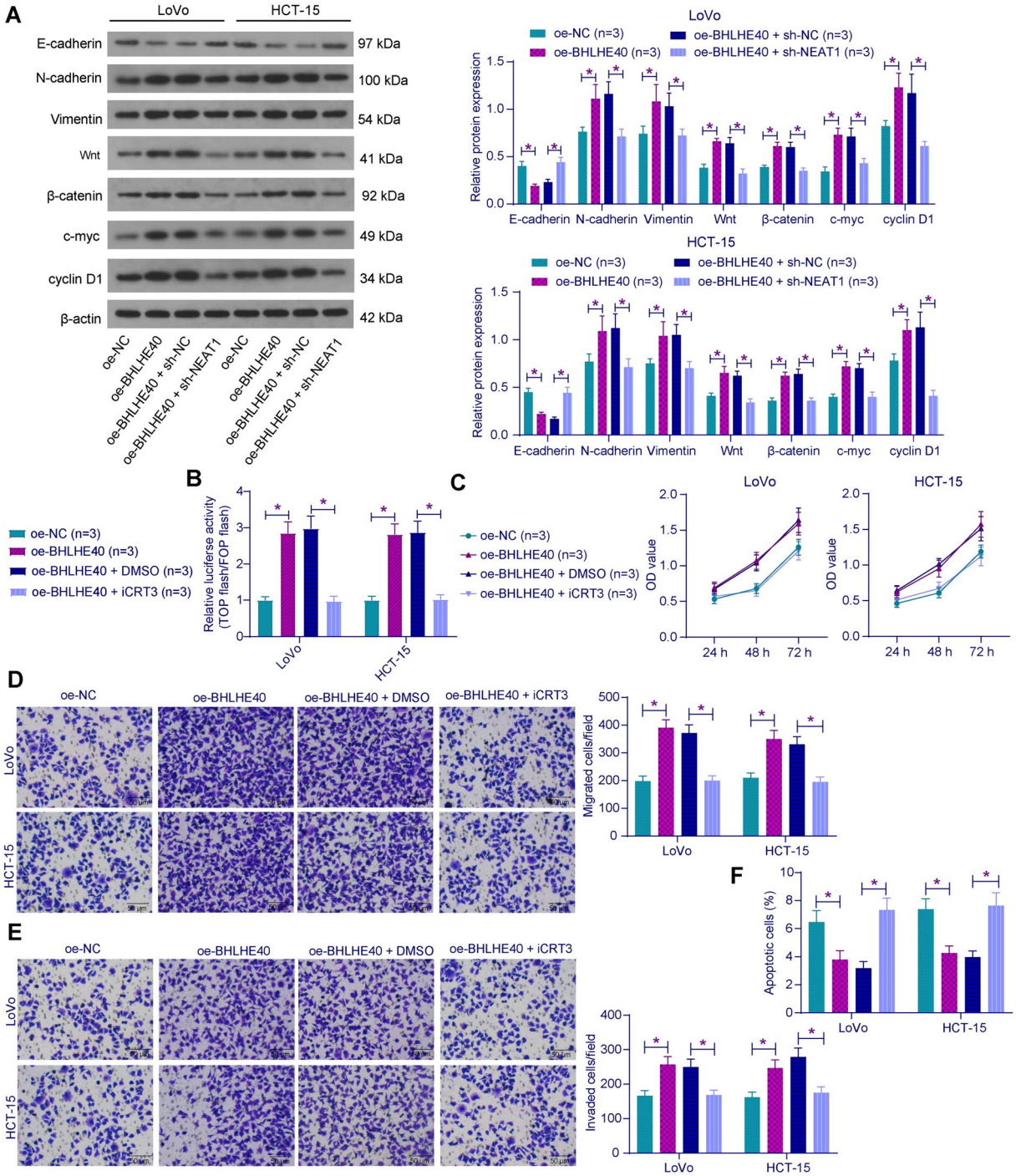

Fig. 5 BHLHE40 mediates NEAT1 transcription to activate Wnt/β-catenin signaling in CRC cells. **A** Western blot for the E-cadherin, N-cadherin, Vimentin, Wnt, β-catenin, c-myc, and cyclin D1 protein expression in CRC cells in response to oe-BHLHE40 (oe-NC as control) or oe-BHLHE40 + sh-NEAT1 (oe-BHLHE40 + sh-NC as control). **B** Effects of oe-BHLHE40 and iCRT3 combined treatment on Wnt/β-catenin pathway activity in CRC cells was measured using TOP/FOP flash assay. **C** MTT assay for LoVo and HCT-15 cell viability. **D** Transwell assay for LoVo and HCT-15 cell migration ability. **E** Transwell assay for LoVo and HCT-15 cell invasion ability. **F** Flow cytometry for LoVo and HCT-15 cell apoptosis. Results were expressed as magnitude of relative expression (means ± SD) from three independent experiments. Two-way ANOVA. *$p < 0.05$

transcription factors in the regulation of NEAT1 due to the complex tumor microenvironments.

It has been shown that higher matrix stiffness triggered NEAT1 expression which activated the Wnt/β-catenin pathway in liver cancer [30]. The promoting effects of NEAT1 on the Wnt/β-catenin pathway have also been validated in CRC [31]. The interaction between the Wnt/β-catenin signaling and EMT has been verified [32] and sustained Wnt/β-catenin signaling activation induces hyperproliferation and oncogenic transformation of intestinal epithelial cells, contributing to CRC onset [33]. Here, we demonstrated that the activating effects of BHLHE40 on the Wnt/β-catenin signaling were reversed by silencing of NEAT1 in CRC cells, further evidencing that NEAT1 was a downstream target of BHLHE40. In addition, the tumor-promoting properties effects of BHLHE40 on CRC cells were mitigated by the Wnt/β-catenin antagonist iCRT3.

Conclusion

In summary, we have shown that BHLHE40 expedites the transcription of NEAT1. This interaction is important for understanding the role played by NEAT1 in the regulation of cell proliferation and EMT. We have also demonstrated that the Wnt/β-catenin signaling is an effector of the BHLHE40/NEAT1 in CRC. Our data provide insights into the molecular mechanisms of EMT in CRC and reveal BHLHE40 and NEAT1 as novel molecular targets for therapeutic strategies of CRC.

Materials and methods

Patient tissues collection

CRC tissues and adjacent normal tissues were harvested from 54 CRC patients who attended the Second Affiliated Hospital of Hainan Medical University from June 2022 to June 2023. Paraffin-embedded tissue sections were obtained from the Pathology Department of the Second Affiliated Hospital of Hainan Medical University. Patients who received chemotherapy, radiotherapy, or any other adjuvant treatment before surgery were excluded from this study, and the histopathology was determined by two pathologists according to World Health Organization criteria. This study was conducted according to the guidelines of the *Declaration of Helsinki* and approved by the Ethics Committee of the Second Affiliated Hospital of Hainan Medical University (approval number: 2023-KCSN-09), and all participants gave informed consent.

Cell culture and treatment

Human colon epithelium cell HCoEpiC (YS1700C, YaJi Biological, Shanghai, China), and human CRC cell lines LoVo (CL-0144), HCT-15 (CL-0097) and Caco-2 (CL-0050, all from Procell, Wuhan, Hubei, China) were used in this study. The cells were activated and cultured in Dulbecco's Modified Eagle's medium (M0101A, WheLab, Shanghai, China) with 10% FBS + 1% penicillin/streptomycin at 37 °C and 5% CO_2.

GenePharma Co., Ltd. (Shanghai, China) synthesized recombinant lentivirus expressing short hairpin RNA (sh)-NEAT1, sh-BHLHE40, sh-negative control (NC), overexpression (oe)-BHLHE40, oe-NEAT1, and oe-NC. LoVo and HCT-15 cells in good growth condition were seeded into 6-well plates, and the lentiviral vector was added for infection when the cell confluence reached about 50%. After a 72-h incubation at 37℃ and 5% CO_2, the infection efficiency was verified by RT-qPCR. The cells were treated with a Wnt/β-catenin signaling antagonist iCRT3 (catalog number: S8647, Selleck, Houston, TX, USA) at a concentration of 75 μM or control DMSO for 24 h.

Cell proliferation assay

Cell proliferation was analyzed using the MTT Cell Proliferation and Cytotoxicity Assay Kit (M1020, Beijing Solarbio Life Sciences Co., Ltd., Beijing, China). The CRC cells were supplemented to a 96-well plate (5000 cells per well) and incubated in an incubator for 24 h, 48 h, or 72 h. After aspiration of the supernatant, 90 μL of fresh medium and 10 μL of MTT solution were supplemented to each well. After 4 h of incubation, the supernatant was aspirated off, and 110 μL of DMSO was supplemented to each well to dissolve the methanogenic crystals. The optical density (OD) value was measured at 490 nm with a microplate reader.

Cell migration and invasion assays

The Transwell chambers were placed in a 24-well plate, and 50 μL of diluted Matrigel was added to the apical chamber (Matrigel was not added during the migration assay). Infected cells (10^5) suspended in serum-free medium were supplemented to the apical chamber, and 500 μL of fresh medium containing 10% FBS was supplemented to the basolateral chamber. After 24 h, cells in the basolateral chamber were fixed using 4% paraformaldehyde, stained using 0.1% crystal violet (A100528, Sangon Biotech, Shanghai, China) staining solution, and counted.

Flow cytometry

LoVo and HCT-15 cells were assayed using Annexin V-fluorescein isothiocyanate (FITC)/propidium iodide (PI) fluorescent dual-stained apoptosis detection kit (E606336, Sangon). The cells were centrifuged at 300 g for 5 min, gently resuspended, and counted. Cells were resuspended by adding diluted 1 × Annexin V Binding Buffer working solution, and 5 μL of Annexin V-FITC and 5 μL of PI staining solution were added to the cell

suspension. The samples were incubated for 15–20 min at room temperature in the dark and loaded immediately after the reaction was completed.

Western blot

Cell precipitates were lysed in RIPA buffer with a proteinase inhibitor. The supernatant was aspirated by centrifugation using a 4 °C centrifuge to extract the total protein. After sodium dodecyl sulfate–polyacrylamide gel electrophoresis, the proteins were transferred onto polyvinylidene fluoride (PVDF) membranes. Afterward, the membranes were sealed with non-fat milk at room temperature for 2 h. Primary antibodies to BHLHE40 (1:1000, 17895-1-AP, ProteinTech Group, Chicago, IL, USA), Wnt (1:500, 27935-1-AP, ProteinTech Group), β-catenin (1:2000, 17565-1-AP, ProteinTech), cyclin D1 (1:5000, 26939-1-AP, ProteinTech), c-myc (1:500, GTX103436, GeneTex, Inc., Alton Pkwy Irvine, CA, USA), E-cadherin (1:500, GTX100443, GeneTex), N-cadherin (1:500, GTX127345, GeneTex), Vimentin (1:5000, GTX100619, GeneTex), and β-actin (1:500, D110001, Sangon) were applied overnight at 4 ℃. After incubated with the horseradish peroxidase (HRP)-labeled goat anti-rabbit (1:1000, GTX213110-01, GeneTex) at room temperature for 1 h, the protein signals were visualized using the ECL system. The grayscale values of the bands were calculated using ImageJ software to determine the expression of the target protein.

RT-qPCR

Total RNA was extracted from cells using Trizol Total RNA Extraction Reagent (Tansoole, Shanghai, China), and miRNeasy FFPE Kit (Qiagen, Valencia, CA, USA) was used to extract total RNA from paraffin-embedded tissue sections. Reverse transcription and PCR were performed according to the instructions of the Reverse Transcription Kit (041088841, Tansoole) and Probe Method Fluorescence PCR Premix (041093363, Tansoole). β-actin was used as the reference gene. The qPCR primer sequences are NEAT1 forward, 5′-AAACGCTGGGAGGGTACAAG-3′, NEAT1 reverse, 5′-ATGCCCAAACTAGACCTGCC-3′, BHLHE40 forward, 5′-CCAGTCATCCAGCGGACTTT-3′, BHLHE40 reverse, 5′-GGGGGTTCTTCGGACTCTTG-3′, β-actin forward, 5′-ACAGAGCCTCGCCTTTGCC-3′, β-actin reverse, 5′-TGGGGTACTTCAGGGTGAGG-3′.

Luciferase reporter assay

The NEAT1 sequence was inserted into the pGL3-Basic luciferase vector (P32227, Miaolingbio. Inc, Wuhan, Hubei, China), and the vector was transfected into sh-NC or sh-BHLHE40 lentivirus-infected LoVo and HCT-15 cells for 24 h. The cells were lysed, and the firefly luciferase and renilla luciferase activities were measured using a dual luciferase assay kit (16186, Thermo Fisher Scientific Inc., Waltham, MA, USA).

TOP flash luciferase reporter gene plasmid (D2501, Beyotime Biotechnology Co., Ltd., Shanghai, China) was used to detect Wnt/β-catenin-mediated TCF/LEF transcriptional activity levels, and FOP flash (D2503, Beyotime) with mutated TCF/LEF binding site sequences was used as a negative control. The above reporter plasmids were transfected into CRC cells by Lipofectamine 2000 (Thermo Fisher). Wnt/β-catenin pathway activity was measured 24 h later by measuring luciferase activity with a dual luciferase assay kit (16186, Thermo Fisher).

Chromatin immunoprecipitation (ChIP) assay

ChIP was performed according to the manufacturer's instructions for the ChIP assay kit (17-295, Sigma-Aldrich Chemical Company, St Louis, MO, US). The cells were first cross-linked with 1% formaldehyde at room temperature for 10 min, quenched with 125 mM glycine for 5 min, and lysed with lysis buffer, followed by sonication to obtain chromatin fragments. Antibodies were coupled to magnetic beads at 4 °C overnight. Chromatin-protein complexes were incubated overnight at 4 °C with BHLHE40 antibody (1:50, PA1-16546, Thermo Fisher) coupled to magnetic beads, and rabbit IgG (Thermo Fisher) was used as a control. The purified DNA samples were quantified by qPCR.

In vivo experiments

Forty-eight BALB/C female nude mice (6 weeks old, weighing 14–17 g) were purchased from Hunan SJA Laboratory Animal Co., Ltd. (Changsha, Hunan, China). This study was approved by the Institutional Animal Care and Use Committee of the Second Affiliated Hospital of Hainan Medical University.

Twenty-four BALB/C nude mice were divided into sh-NC, sh-BHLHE40, sh-BHLHE40 + oe-NC and sh-BHLHE40 + oe-NEAT1 groups (n = 6/group). After the mice were fully anesthetized, 100 μL of HCT-15 cell suspension (containing ~ 10^7 cells) infected with the respective lentivirus was injected subcutaneously. Mice were monitored for status (body weight, water intake, excretion and activity, fur gloss) and growth of subcutaneous tumors in the lateral abdomen. When the tumor formed a visible bulge, the long axis L (mm) and short axis W (mm) of the tumor were measured weekly with vernier calipers to calculate the volume of the tumor using the formula: volume = $L \times W^2/2$. Four weeks later, the mice were euthanized with an overdose of anesthetic in an ultra-clean table to remove the tumors.

The remaining 24 BALB/C nude mice were divided into four groups as above mentioned as well (n = 6/group).

HCT-15 cells in logarithmic phase and good growth condition were taken for the experiment. After anesthetizing the mice, approximately 10^6 lentivirus-infected HCT-15 cells in 100 μL of suspension were injected via the tail vein. The mice were euthanized with an overdose of anesthetic 24 days later, and the lungs were carefully removed for fixation and embedding for subsequent hematoxylin-eosin (HE) staining.

HE staining

Lung tissue sections were dewaxed by immersion in xylene and rehydrated by adding different concentrations of ethanol for 5 min. The sections were stained with hematoxylin staining solution for 5 min, treated in 0.5% hydrochloric acid alcohol for 20 s, and stained with 0.1–0.5% eosin staining solution for 2 min, followed by rinsing with distilled water. Dehydration and clearing were performed in ethanol and xylene, and the sections were sealed with drops of neutral gum and observed under a light microscope.

Immunohistochemical analysis

Xenograft tumor tissue sections were sequentially soaked in xylene and ethanol for dewaxing and hydration, and heated with citrate buffer for antigen retrieval. The addition of 3% hydrogen peroxide was used to eliminate endogenous peroxidase activity. The sections were sealed with 5% FBS for half an hour and incubated with diluted antibodies to Ki67 (1:100, SAB5700770-100UL, Sigma) and BHLHE40 (1:100, PA1-16546, Thermo Fisher) overnight at 4 °C and with HRP-labeled goat anti-rabbit (1:1000, A0208, Beyotime) secondary antibody for 60 min. The color was developed with a DAB kit (P0202, Beyotime), and hematoxylin was used for counter-staining. The sections were dehydrated and cleared in ethanol and xylene, sealed with a drop of neutral gum, and placed under an inverted microscope for observation.

Statistics

Statistical analyses were performed using GraphPad Prism 8 (GraphPad, San Diego, CA, USA). Data were shown as mean ± SD. One-way ANOVA, two-way ANOVA, and paired t-tests were used to compare the differences between groups. Three independent biological repetitions were carried out for each assay. Statistical significance was indicated when p-values were less than 0.05.

Abbreviations

CRC	Colorectal cancer
NEAT1	Nuclear-enriched abundant transcript 1
BHLHE40	Class E basic helix-loop-helix protein 40
FBS	Fetal bovine serum
sh	Short hairpin RNA
NC	Negative control
FITC	Fluorescein isothiocyanate
PI	Propidium iodide
HRP	Horseradish peroxidase
ChIP	Chromatin immunoprecipitation
HE	Hematoxylin–eosin

Author contributions

ALJ was responsible for the design of the study, data analysis, and manuscript writing. HL contributed to data acquisition, analysis, and interpretation, and also drafted and critically revised the manuscript. XWF contributed to the analysis and interpretation of the data. YRZ and YHL contributed to the data collection, statistical analysis, and manuscript review. All authors read and approved the final manuscript.

Funding

This work was supported by the Hainan Health Industry Scientific Research Project (21A200277) and the Project supported by Hainan Province Clinical Medical Center.

Data availability

This published article includes all the data generated or analyzed during this study.

Declarations

Ethics approval and consent to participate

This study was conducted according to the guidelines of the *Declaration of Helsinki* and approved by the Ethics Committee of the Second Affiliated Hospital of Hainan Medical University (approval number: 2023-KCSN-09), written informed consent for publication was obtained from all participants. Animal experiment was approved by the Institutional Animal Care and Use Committee of the Second Affiliated Hospital of Hainan Medical University.

Consent for publication

All authors read the journal's guidelines and agreed with consent for publication.

Competing interests

The authors declare that they have no potential conflict of interest.

Received: 31 January 2024 Accepted: 22 July 2024
Published online: 04 August 2024

References

1. Dekker E, Tanis PJ, Vleugels JLA, Kasi PM, Wallace MB. Colorectal cancer. Lancet. 2019;394(10207):1467–80. https://doi.org/10.1016/S0140-6736(19)32319-0.
2. Miller KD, Nogueira L, Devasia T, Mariotto AB, Yabroff KR, Jemal A, et al. Cancer treatment and survivorship statistics, 2022. CA Cancer J Clin. 2022;72(5):409–36. https://doi.org/10.3322/caac.21731.
3. Siegel RL, Miller KD, Goding Sauer A, Fedewa SA, Butterly LF, Anderson JC, et al. Colorectal cancer statistics, 2020. CA Cancer J Clin. 2020;70(3):145–64. https://doi.org/10.3322/caac.21601.
4. Vu T, Datta PK. Regulation of EMT in colorectal cancer: a culprit in metastasis. Cancers (Basel). 2017. https://doi.org/10.3390/cancers9120171.
5. Zhang N, Ng AS, Cai S, Li Q, Yang L, Kerr D. Novel therapeutic strategies: targeting epithelial-mesenchymal transition in colorectal cancer. Lancet Oncol. 2021;22(8):e358–68. https://doi.org/10.1016/S1470-2045(21)00343-0.
6. Loganathan T, Doss CG. Non-coding RNAs in human health and disease: potential function as biomarkers and therapeutic targets. Funct Integr Genom. 2023;23(1):33. https://doi.org/10.1007/s10142-022-00947-4.
7. Lee YJ, Kim WR, Park EG, Lee DH, Kim JM, Shin HJ, et al. Exploring the key signaling pathways and ncRNAs in colorectal cancer. Int J Mol Sci. 2024. https://doi.org/10.3390/ijms25084548.

8. Chen S, Shen X. Long noncoding RNAs: functions and mechanisms in colon cancer. Mol Cancer. 2020;19(1):167. https://doi.org/10.1186/s12943-020-01287-2.
9. Li K, Yao T, Zhang Y, Li W, Wang Z. NEAT1 as a competing endogenous RNA in tumorigenesis of various cancers: Role, mechanism, and therapeutic potential. Int J Biol Sci. 2021;17(13):3428–40. https://doi.org/10.7150/ijbs.62728.
10. Zhou WJ, Wang HY, Zhang J, Dai HY, Yao ZX, Zheng Z, et al. NEAT1/miR-200b-3p/SMAD2 axis promotes progression of melanoma. Aging (Albany NY). 2020;12(22):22759–75. https://doi.org/10.18632/aging.103909.
11. Azizidoost S, Ghaedrahmati F, Anbiyaee O, Ahmad Ali R, Cheraghzadeh M, Farzaneh M. Emerging roles for lncRNA-NEAT1 in colorectal cancer. Cancer Cell Int. 2022;22(1):209. https://doi.org/10.1186/s12935-022-02627-6.
12. Zhang M, Weng W, Zhang Q, Wu Y, Ni S, Tan C, et al. The lncRNA NEAT1 activates Wnt/beta-catenin signaling and promotes colorectal cancer progression via interacting with DDX5. J Hematol Oncol. 2018;11(1):113. https://doi.org/10.1186/s13045-018-0656-7.
13. Papathanasiou I, Balis C, Destounis D, Mourmoura E, Tsezou A. NEAT1-mediated miR-150-5p downregulation regulates b-catenin expression in OA chondrocytes. Funct Integr Genom. 2023;23(3):246. https://doi.org/10.1007/s10142-023-01139-4.
14. Zhao H, Ming T, Tang S, Ren S, Yang H, Liu M, et al. Wnt signaling in colorectal cancer: pathogenic role and therapeutic target. Mol Cancer. 2022;21(1):144. https://doi.org/10.1186/s12943-022-01616-7.
15. Xu Q, Li X, Li Y, Yu J, Yang A. Kinesin family member 23 knockdown inhibits cell proliferation and epithelial-mesenchymal transition in esophageal carcinoma by inactivating the Wnt/beta-catenin pathway. Funct Integr Genom. 2023;23(2):154. https://doi.org/10.1007/s10142-023-01088-y.
16. Wang Z, Li K, Huang W. Long non-coding RNA NEAT1-centric gene regulation. Cell Mol Life Sci. 2020;77(19):3769–79. https://doi.org/10.1007/s00018-020-03503-0.
17. Wang L, Cho KB, Li Y, Tao G, Xie Z, Guo B. Long noncoding RNA (lncRNA)-mediated competing endogenous RNA networks provide novel potential biomarkers and therapeutic targets for colorectal cancer. Int J Mol Sci. 2019. https://doi.org/10.3390/ijms20225758.
18. Xu D, Dong P, Xiong Y, Yue J, Konno Y, Ihira K, et al. MicroRNA-361-mediated inhibition of HSP90 expression and EMT in cervical cancer is counteracted by oncogenic lncRNA NEAT1. Cells. 2020. https://doi.org/10.3390/cells9030632.
19. Wen S, Wei Y, Zen C, Xiong W, Niu Y, Zhao Y. Long non-coding RNA NEAT1 promotes bone metastasis of prostate cancer through N6-methyladenosine. Mol Cancer. 2020;19(1):171. https://doi.org/10.1186/s12943-020-01293-4.
20. Cook ME, Jarjour NN, Lin CC, Edelson BT. Transcription factor Bhlhe40 in immunity and autoimmunity. Trend Immunol. 2020;41(11):1023–36. https://doi.org/10.1016/j.it.2020.09.002.
21. Wang J, Li B, Yang S, Ma C, Liu K, Chen X, et al. Upregulation of INHBA mediated by the transcription factor BHLHE40 promotes colon cancer cell proliferation and migration. J Clin Lab Anal. 2022;36(7): e24539. https://doi.org/10.1002/jcla.24539.
22. Wang W, Reiser-Erkan C, Michalski CW, Raggi MC, Quan L, Yupei Z, et al. Hypoxia inducible BHLHB2 is a novel and independent prognostic marker in pancreatic ductal adenocarcinoma. Biochem Biophys Res Commun. 2010;401(3):422–8. https://doi.org/10.1016/j.bbrc.2010.09.070.
23. Shan E, Huo Y, Wang H, Zhang Z, Hu J, Wang G, et al. Differentiated embryonic chondrocyte expressed gene-1 (DEC1) enhances the development of colorectal cancer with an involvement of the STAT3 signaling. Neoplasia. 2022;27: 100783. https://doi.org/10.1016/j.neo.2022.100783.
24. Zheng Q, Wang C, Wang L, Zhang D, Liu N, Ming X, et al. Interaction with SP1, but not binding to the E-box motifs, is responsible for BHLHE40/DEC1-induced transcriptional suppression of CLDN1 and cell invasion in MCF-7 cells. Mol Carcinog. 2018;57(9):1116–29. https://doi.org/10.1002/mc.22829.
25. Xiong J, Yang H, Luo W, Shan E, Liu J, Zhang F, et al. The anti-metastatic effect of 8-MOP on hepatocellular carcinoma is potentiated by the down-regulation of bHLH transcription factor DEC1. Pharmacol Res. 2016;105:121–33. https://doi.org/10.1016/j.phrs.2016.01.025.
26. Sethuraman A, Brown M, Krutilina R, Wu ZH, Seagroves TN, Pfeffer LM, et al. BHLHE40 confers a pro-survival and pro-metastatic phenotype to breast cancer cells by modulating HBEGF secretion. Breast Cancer Res. 2018;20(1):117. https://doi.org/10.1186/s13058-018-1046-3.
27. Wu Y, Sato F, Yamada T, Bhawal UK, Kawamoto T, Fujimoto K, et al. The BHLH transcription factor DEC1 plays an important role in the epithelial-mesenchymal transition of pancreatic cancer. Int J Oncol. 2012;41(4):1337–46. https://doi.org/10.3892/ijo.2012.1559.
28. Wang X, Jiang G, Ren W, Wang B, Yang C, Li M. LncRNA NEAT1 regulates 5-Fu sensitivity, apoptosis and invasion in colorectal cancer through the MiR-150-5p/CPSF4 axis. Onco Target Ther. 2020;13:6373–83. https://doi.org/10.2147/OTT.S239432.
29. Fu X, Deng X, Xiao W, Huang B, Yi X, Zou Y. Downregulation of NEAT1 sensitizes gemcitabine-resistant pancreatic cancer cells to gemcitabine through modulation of the miR-506-3p/ZEB2/EMT axis. Am J Cancer Res. 2021;11(8):3841–56.
30. Xu X, Zhang Y, Wang X, Li S, Tang L. Substrate stiffness drives epithelial to mesenchymal transition and proliferation through the NEAT1-Wnt/beta-catenin pathway in liver cancer. Int J Mol Sci. 2021. https://doi.org/10.3390/ijms222112066.
31. Liu Z, Gu Y, Cheng X, Jiang H, Huang Y, Zhang Y, et al. Upregulation lncNEAT1 contributes to colorectal cancer progression through sponging miR-486-5p and activating NR4A1/Wnt/beta-catenin pathway. Cancer Biomark. 2021;30(3):309–19. https://doi.org/10.3233/CBM-201733.
32. Fang F, Jin X, Meng J, He J, Wang J, Wang C, et al. Jiedu Fuzheng decoction improves the proliferation, migration, invasion and EMT of non-small cell lung cancer via the Wnt/beta-catenin pathway. Cell Div. 2023;18(1):22. https://doi.org/10.1186/s13008-023-00105-7.
33. Prossomariti A, Piazzi G, Alquati C, Ricciardiello L. Are Wnt/beta-catenin and PI3K/AKT/mTORC1 distinct pathways in colorectal cancer? Cell Mol Gastroenterol Hepatol. 2020;10(3):491–506. https://doi.org/10.1016/j.jcmgh.2020.04.007.

Publisher's Note